Chemical Science

EDGE ARTICLE

View Article Online
View Journal | View Issue

Cite this: *Chem. Sci.*, 2017, **8**, 8279

Fluoro-substituted cyanine for reliable *in vivo* labelling of amyloid-β oligomers and neuroprotection against amyloid-β induced toxicity†

Yinhui Li,‡[ac] Di Xu,‡[c] Anyang Sun,‡*[b] See-Lok Ho,‡[c] Chung-Yan Poon,[c] Hei-Nga Chan,[c] Olivia T. W. Ng,[d] Ken K. L. Yung,[d] Hui Yan,[e] Hung-Wing Li *[c] and Man Shing Wong *[c]

Alzheimer's disease (AD) is the most prevalent but still incurable neurodegenerative form of dementia. Early diagnosis and intervention are crucial for delaying the onset and progression of the disease. We herein report a novel fluoro-substituted cyanine, F-SLOH, which exhibits good Aβ oligomer selectivity with a high binding affinity, attributed to the synergistic effect of strong π–π stacking and intermolecular CH···O and CH···F interactions. The selectivity towards the Aβ oligomers in the brain was ascertained by *in vitro* labelling on tissue sections and *in vivo* labelling through the systemic administration of F-SLOH in 7 month APP/PS1 double transgenic (Tg) and APP/PS1/Tau triple Tg mouse models. F-SLOH also shows remarkably effective inhibition on Aβ aggregation and highly desirable neuroprotective effects against Aβ-induced toxicities, including the inhibition of ROS production and Ca^{2+} influx. Its excellent blood–brain barrier (BBB) penetrability and low bio-toxicity further support its tremendous potential as a novel theranostic agent for both early diagnosis and therapy of AD.

Received 11th September 2017
Accepted 4th October 2017

DOI: 10.1039/c7sc03974c

rsc.li/chemical-science

Introduction

Alzheimer's disease (AD) is the most prevalent neurodegenerative disease, commonly found amongst the elderly.[1,2] Unfortunately, AD is still incurable and the underlying cause is also not yet known, which poses a grand challenge for the development of effective diagnostic tools and treatment for this devastating disease.[3,4] An amyloid-β (Aβ) plaque is one of the important pathological hallmarks in an AD brain,[5,6] and a number of probes for imaging the Aβ plaques as a biomarker have been reported over the years. Despite all of these efforts, only few contrast agents for various advanced molecular imaging techniques[7–11] have been approved for clinical diagnostics. In fact, the formation of Aβ plaques in the brain reflects a dynamic equilibrium and an interplay among the Aβ monomers, oligomers and fibrils.[12] Studies indicate that the deposition of Aβ plaques does not correlate with the disease progression of AD but soluble Aβ oligomers are believed to play a detrimental role in the cause of the disease.[13] Thus, early diagnosis and intervention are much more crucial for delaying disease progression and preventing irreversible neuronal damage.

Increasing evidence suggests that soluble oligomeric Aβ is a major cause of cytotoxicities such as induction of oxidative stress and elevations of intracellular [Ca^{2+}] in the pathological cascade of AD.[14,15] In addition, Aβ oligomers are more neurotoxic than insoluble Aβ fibrils in the plaques, and are responsible for the dysfunction of neurotransmission, and the imbalance of neuronal excitability, eventually resulting in neuronal death and memory impairment. Aβ oligomer formation and deposition could represent one of the appropriate biomarkers for early AD diagnosis; and their dynamic levels in the brain could be considered as one of the key indicators in evaluating the disease progression.[12,16,17] Thus, development of a reliable method to selectively detect Aβ oligomers and suppress oligomer formation before the onset of clinical symptoms is highly desirable and beneficial in early diagnostics and therapeutics of AD.

Nevertheless, chemical probes developed over the past decades mainly detected insoluble Aβ species and had poor

[a]*Key Laboratory for Green Organic Synthesis and Application of Hunan Province, Key Laboratory of Environmentally Friendly Chemistry, Application of Ministry of Education, College of Chemistry, Xiangtan University, Xiangtan, 411105, China*

[b]*Laboratory of Neurodegenerative Diseases and Molecular Imaging, Shanghai University of Medicine & Health Sciences, Shanghai, 201318, China. E-mail: sunay@sumhs.edu.cn*

[c]*Department of Chemistry, Hong Kong Baptist University, Kowloon Tong, Hong Kong SAR, China. E-mail: mswong@hkbu.edu.hk; hwli@hkbu.edu.hk*

[d]*Department of Biology, Hong Kong Baptist University, Kowloon Tong, Hong Kong SAR, China*

[e]*School of Pharmacy, Liaocheng University, Liaochen, 252059, China*

† Electronic supplementary information (ESI) available. See DOI: 10.1039/c7sc03974c

‡ These authors contributed equally to this work.

selectivity towards soluble Aβ oligomers.[18,19] This is due to the lack of guidelines for designing imaging probes for the selective recognition of soluble Aβ oligomers because of the heterogeneous and transient nature of oligomers. Viola *et al.* have developed an MRI probe for selective recognition of Aβ oligomers by incorporating oligomer-specific antibodies onto magnetic nanostructures.[20] On the other hand, fluorescence imaging offers a rapid, real-time and sensitive diagnostic alternative,[21] which is powerful for monitoring the dynamic progress of Aβ peptide aggregation and fibrillogenesis. Although a few Aβ oligomer imaging probes have recently been reported, they are not effective and sensitive enough for Aβ oligomer detection and imaging *ex vivo* and *in vivo*. For instance, BD-Oligo shows very poor BBB permeability and was applied only in the imaging of mature APP × PS1 Tg mice.[22] ANSP possesses only a moderate binding affinity to Aβ oligomers.[23] *In vivo* detection of Aβ oligomers in Tg mice at a young age when AD-like pathology is just forming has not yet been demonstrated. Thus, the development of an effective and reliable Aβ oligomer targeting probe that is useful for multiple AD mouse models is still a great challenge.

Cyanine dye, a versatile class of turn-on fluorescence probe for two-photon excited imaging, generally exhibits much stronger binding interactions with Aβ fibrils than oligomers and monomers.[24,25] We report herein our new findings on an oligomer-selective cyanine probe, namely F-SLOH. With a fluorine group incorporated into the cyanine lead structure, the probe remarkably becomes highly selective for Aβ oligomeric assemblies with a high binding affinity over monomers or fibrils due to the strong hydrophobic and intermolecular hydrogen bonding interactions, as revealed by molecular docking calculations. Its *in vivo* application in labelling Aβ oligomers was successfully demonstrated in 7 month-old APP/PS1 double Tg and APP/PS1/Tau triple Tg mouse models. Intriguingly, F-SLOH was found not only to show excellent blood–brain barrier penetrability, low bio-toxicity, and a good inhibitory effect on the self-aggregation of Aβ monomers, but also to prevent Aβ-induced toxicities, making it highly useful for *in vivo* applications particularly for early diagnosis and treatment of AD.

Results and discussion

The synthesis of F-SLOH is outlined in Scheme S1† and its structure (Fig. 1A) was confirmed by ^{1}H and ^{13}C NMR spectroscopy as well as high-resolution mass spectroscopy. The photophysical properties of F-SLOH are summarized in Fig. S1.† The absorption and emission spectra showed a large Stokes shift up to 150 nm in PBS solution, which is favorable to avoiding self-absorption in bio-imaging. Although F-SLOH shows weak fluorescence with very low quantum yield ($\Phi_{\lambda=488\ nm}$ = 0.006 in PBS, $\Phi_{\lambda=488\ nm}$ = 0.011 in DMSO), it exhibits different extents of fluorescence enhancement towards the monomers, oligomers and fibrils accompanied by a substantial blue shift of the emission maximum upon an addition of various $A\beta_{1-40}$ species (Fig. 1B), which is attributed to the restricted rotation of the photo-excited dye upon binding to the Aβ species, resulting in a reduction in the non-radiative

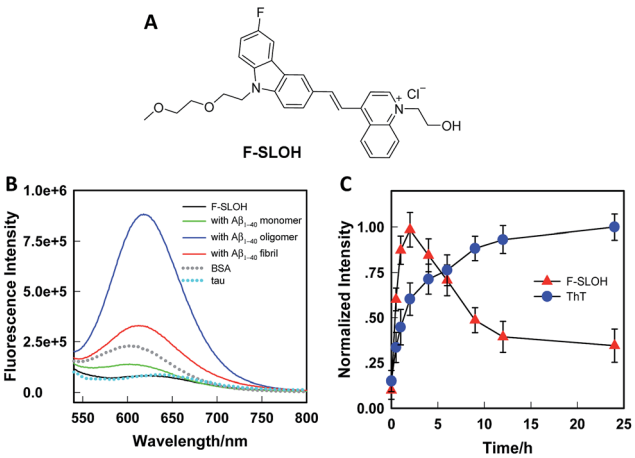

Fig. 1 (A) Molecular structure of F-SLOH. (B) Fluorescence spectra of F-SLOH (1.0 μM) in the presence of 10.0 μM $A\beta_{1-40}$ species (monomers, oligomers and fibrils), BSA and Tau. (C) Monitoring of the growth process of $A\beta_{1-40}$ at different time points by labelling with ThT and F-SLOH, where the fluorescence intensities of ThT and F-SLOH were recorded at 490 and 620 nm, respectively.

decay. Intriguingly, F-SLOH exhibits a stronger fluorescence enhancement upon binding to the Aβ oligomers compared to binding to the monomers and fibrils, giving rise to an enhanced quantum yield of 0.26 which is higher than that of its parent compound, SLOH (Φ = 0.12) (Fig. S2†). Favorably, F-SLOH affords very minor fluorescence enhancement and negligible interference upon mixing/interacting with bovine serum albumin (BSA) and Tau protein, respectively. Considering that the viscosity of the biological medium was about 3.5 cP, which might result in the reduction of non-radiative decay, the effect of the viscosity on the fluorescence of F-SLOH was also investigated. As shown in Fig. S3,† the fluorescence of F-SLOH in a solution of water-glycerol with a viscosity of 4.5 cP is indeed increased, but to a much smaller extent compared to that upon an addition of Aβ. To quantify the binding affinity of Aβ species, the dissociation constant (K_d) of F-SLOH was determined by fluorescence titration (Fig. S4†) and estimated from a Scatchard plot, yielding K_d values of 3.22, 0.66, and 1.90 μM for the monomers, oligomers and fibrils, respectively (Fig. S5†). Such a low K_d value for the oligomer (0.66 μM) indicated that F-SLOH possessed a significantly stronger binding affinity towards Aβ oligomers than monomers and fibrils. Furthermore, a good linearity was obtained in the enhanced fluorescence as a function of the amount of Aβ oligomers added to the F-SLOH solution (Fig. S6†), suggesting its capability for quantitative analysis. In addition, the fluorescence intensity of F-SLOH remains relatively constant over time and over a wide range of pH values (pH = 4–10) (Fig. S7†), indicating its potential for practical applications.

The binding behavior of F-SLOH towards different sizes of $A\beta_{1-40}$ species was also investigated. Different sizes of $A\beta_{1-40}$ species were prepared by incubating the monomer for different durations. Besides recording the emission spectra of F-SLOH, the growth process of Aβ was monitored by ThT staining. As

shown in Fig. 1C, there is a strong increase in the fluorescence of F-SLOH upon binding with Aβ, following incubation in the first 2 h. After reaching a maximum at 2 h of incubation, the enhanced fluorescence decreases in intensity with a longer period of incubation. In contrast, the fluorescence of ThT increased hyperbolically with respect to the incubation time and became saturated when Aβ was incubated for more than 10 h. These results clearly demonstrated that the fluorescence enhancement of F-SLOH by Aβ species is size-dependent and Aβ oligomers afford a stronger fluorescence enhancement than fibrils and monomers upon binding with F-SLOH. The morphology and size of $A\beta_{1-40}$ at selected time points were confirmed by TEM (Fig. S8†) and DLS (Fig. S9†), respectively. The size of the monomeric $A\beta_{1-40}$ is ~22 nm and it gradually increased to 196, 317, 567, and 712 nm after incubation for 1, 2, 4, and 6 h, respectively (Fig. S7†). Thus, F-SLOH displayed a stronger fluorescence enhancement upon binding with an $A\beta_{1-40}$ oligomer with a size smaller than 300 nm.

The confirmational change of the $A\beta_{1-40}$ species upon binding to F-SLOH was elucidated by circular dichroism (CD). As depicted in Fig. S10,† when the monomeric form of $A\beta_{1-40}$ underwent self-aggregation to the fibrillary form, the positive peak at 185 nm diminished and the negative peak showed an obvious red shift from 205 to 223 nm. Such changes indicated a conformational change of the monomeric $A\beta_{1-40}$ from a random coil to a β-sheet and then aggregation to fibrils.[26] Upon binding to F-SLOH, the peak distinctly shifted with a decrease in amplitude. It is worth mentioning that the apparent change in the CD spectrum of the monomers upon incubating with F-SLOH supports the idea that F-SLOH is able to promote structural transformation during $A\beta_{1-40}$ aggregation and inhibit oligomerization and fibrillation. The inhibition effect was further confirmed by a ThT fluorescence assay. The seed-mediated growth of $A\beta_{1-40}$ in the presence of one equivalent of F-SLOH after 12 h incubation exhibited no observable changes in size (Fig. S11†) and nearly no fluorescence response at the emission maximum of ThT (Fig. S12†), suggesting an effective inhibition effect of F-SLOH towards the $A\beta_{1-40}$ monomers. More interestingly, we found that the growth was terminated instantly when F-SLOH was added at any time during the fibrosis process, by measuring the fibril length (Fig. S13†). $A\beta_{1-40}$ is the most abundant species in an AD brain, while $A\beta_{1-42}$ is considered as the most toxic form.[27] We also investigated the inhibition capability of F-SLOH on $A\beta_{1-42}$ oligomerization by performing sodium dodecyl sulfate-poly-acrylamide gel electrophoresis (SDS-PAGE). The results shown in Fig. S14† confirmed that negligible oligomers or fibrils were formed upon the addition of F-SLOH.

To gain insight into the structural features of F-SLOH for the selective binding to the Aβ oligomer, we carried out quantum mechanical calculations of F-SLOH and SLOH (without F-substitution), followed by a molecular docking search and molecular dynamic simulation calculations for both of the assemblies of F-SLOH and SLOH with the Aβ oligomer (Fig. S15†). Their optimized molecular structures were first determined using quantum mechanical calculations at the B3LYP/6-31G* level (Fig. S15A and B†). A well-known Aβ trimer model from the RCSB database (PDB ID: 4NTR)[28] was adopted as the closest working model of an Aβ oligomer available for the binding studies, although it may not completely represent the true picture of the oligomer structure. It was shown that the hydrophobic F19/V36 residues of the Aβ oligomer constitute an oligomer specific binding site (Fig. S15C†).[22,23] This site would only be exposed to solvent in Aβ oligomers but not in Aβ fibrils. Such a unique structural feature of the Aβ oligomer can be used to identify the specific oligomeric probe. As shown in Fig. S15D–G,† both molecules conform to a slightly twisted geometry to maximize the interactions with the Aβ oligomer in which both carbazole moieties of SLOH and F-SLOH are well accommodated by the F19 residue in the Aβ oligomer due to favorable π–π stacking interactions. In the F-SLOH-Aβ oligomer assembly, the quinolinium ring shows close contact with the hydrophobic domain of the Aβ oligomer, and the hydroxyethyl chain on the quinolinium ring also forms a CH···O interaction with the side chain of the V36 residue. However, these types of interactions are not found in the complex of SLOH and the Aβ oligomer. Meanwhile, the fluorine substituent on the carbazole ring also gives rises to the CH···F interaction with the F19 side chain upon binding. As a result, the much higher affinity of F-SLOH towards the Aβ oligomer could be attributed to the strong hydrophobic and intermolecular CH···O and CH···F interactions between F-SLOH and the Aβ oligomer, offering important guidelines for designing Aβ oligomer sensing probes.

The cytotoxicity was evaluated by MTT assays on SH-SY5Y cells. As shown in Fig. 2A, in the presence of F-SLOH, the cell viability is still maintained at a high level, in which its LC_{50} was

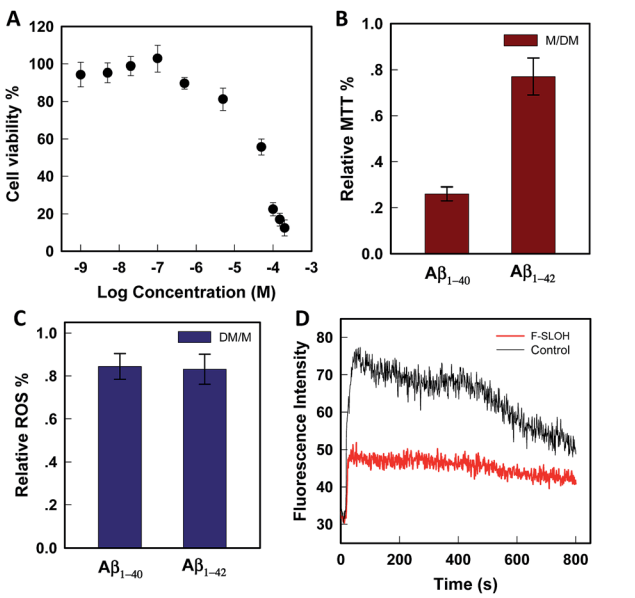

Fig. 2 (A) Cell viability as a function of applied concentration of F-SLOH on the cell-line of SH-SY5Y. (B) MTT assays for evaluating the toxicity as induced by $A\beta_{1-40}$ and $A\beta_{1-42}$ on primary hippocampus neuronal cells in the presence of F-SLOH. (C) Measurement of the ROS level of primary hippocampus neuronal cells under the co-incubation with $A\beta_{1-40}$ and $A\beta_{1-42}$ for 24 h. (D) Fluorescence monitoring of the calcium influx in neuron cells by pre-treatment of F-SLOH.

estimated to be 49 μM. In addition to being non-toxic, F-SLOH showed a pronounced neuroprotective effect on primary neuronal cells against Aβ-induced toxicity. Fig. 2B shows that the toxicity induced by $A\beta_{1-40}$ and $A\beta_{1-42}$ on primary hippocampus neuronal cells is largely reduced by ~25–75% upon the addition of F-SLOH, leading to greatly enhanced cell viabilities. It is well-known that ROS generation and Ca(II) ion overloading are two of the toxic effects induced by Aβ species. Here, we found that F-SLOH could reduce the ROS production induced by both $A\beta_{1-40}$ and $A\beta_{1-42}$ on primary hippocampus neuronal cells. As depicted in Fig. 2C, F-SLOH reduces the level of ROS of primary hippocampus neuronal cells by 15–20% under co-incubation with $A\beta_{1-40}$ and $A\beta_{1-42}$. Furthermore, as shown in Fig. 2D, $A\beta_{1-42}$ would induce a significant level of calcium influx into the neuron cells; however, the calcium uploading was almost reduced to half in the F-SLOH pre-treated primary neuronal cells, compared to that of the control. The excellent neuroprotective effect of F-SLOH against ROS generation and calcium influx further highlights its great potential for therapeutics of AD.

The practical application of F-SLOH for specific detection and labelling of Aβ oligomers in Tg mouse brain tissue was investigated by colocalization studies. A triple Tg AD model (APP/PS1/Tau) was used to examine the colocalization of F-SLOH labelling and Aβ or Tau immunoreactivity. When F-SLOH was incubated with brain slices of Tg and wild-type (WT) mice, distinct contrasts of the plaque-like fluorescence images in the brain section of the Tg mouse, but little fluorescence in the WT brain, were observed (Fig. S16†). These results suggested that F-SLOH was able to label the Aβ species in the AD Tg mouse model. Moreover, the growth in size and the counts of existing plaques in the Tg mice of the two age groups (7 month and 10 month) were obviously visualized (Fig. S17†). When the brain slices were co-stained with SLOH, F-SLOH and the Aβ-fibril tracker thioflavin-S (Thio-S), remarkable differences were observed, in which SLOH and Thio-S only stained in the central core of the plaques while F-SLOH could label not only the core but also the peripheral areas of the plaques (Fig. S17 and S18†). In addition, the staining with Thio-S shows a higher degree of colocalization with SLOH than with F-SLOH. All these results indicate that F-SLOH is capable of staining the transient, unstable oligomer species present in the transition to fibril elongation. The targeting selectivity towards oligomers of F-SLOH was further verified using various antibodies including an Aβ oligomer-specific antibody (Aβ-Oligo), Aβ monomer antibodies (6E10 or 4G8), a total Aβ antibody (pAβ) and a conformational Tau antibody (MC1). Fig. 3 shows that the fluorescence of F-SLOH exhibited excellent colocalization with the immunofluorescence of Aβ-Oligo. On the other hand, the stained areas of 4G8, 6E10 and pAβ were much more extensive than those of Aβ-Oligo and F-SLOH, due to the fact that these three antibodies recognize more forms of Aβ. 4G8 and 6E10 also labelled a subset of neurons (arrowheads) where Aβ monomers could be present. No overlay was found between the F-SLOH labelling and MC1 (for the Tau protein) immunofluorescence. All these results consistently ascertained the specific staining ability of F-SLOH for Aβ oligomers in the brain sections of AD mouse models.

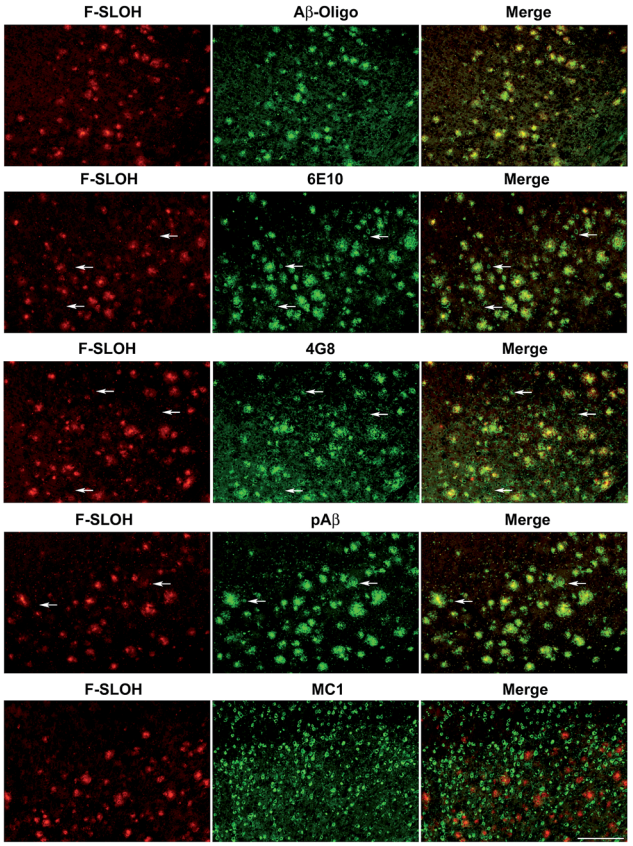

Fig. 3 *In vitro* colocalization analyses of F-SLOH labelling and immunoreactivities of various Aβ species in an AD transgenic mouse model. Brain sections of Tg mice (APP/PS1/Tau, 10 month old) were labelled first with F-SLOH (1.0 μM), followed by incubation with a primary antibody (Aβ-Oligo, 6E10, 4G8, pAβ, or MC1) and a secondary antibody conjugated with Alexa 488. Scale bar: 200 μm.

The blood–brain barrier (BBB) permeability is a prerequisite for any *in vivo* applications. The index of lipophilicity (log *P*) of F-SLOH was first determined to be 2.5 using the online ALOGPS 2.1 program. It is regarded as highly desirable for BBB penetration. The BBB permeability and the washout rate from the brain with F-SLOH were then investigated by *in vivo* imaging analysis. The 7 month-old AD Tg and age-matched WT mice as a control were injected with F-SLOH *via* the tail vein at a dosage of 5.0 mg kg^{-1}. As shown in Fig. S19A,† a remarkably bright fluorescence signal of F-SLOH was observed in the brains of both the Tg and WT mice within 10 min, compared to that of the pre-injected mouse, indicating that F-SLOH was indeed BBB penetrable with a high initial brain uptake. The fluorescence signals in the brain diminished significantly over time, but the decline rate was considerably slower in the Tg mouse compared to that in the WT mouse. This was due to the presence of Aβ species in the Tg mice which strongly bind to F-SLOH, leading to a decrease of outflow rate. Then, the brain kinetic profiles by semi-quantitative analysis of the fluorescence images of the brains were estimated at a region of interest (ROI). Significantly

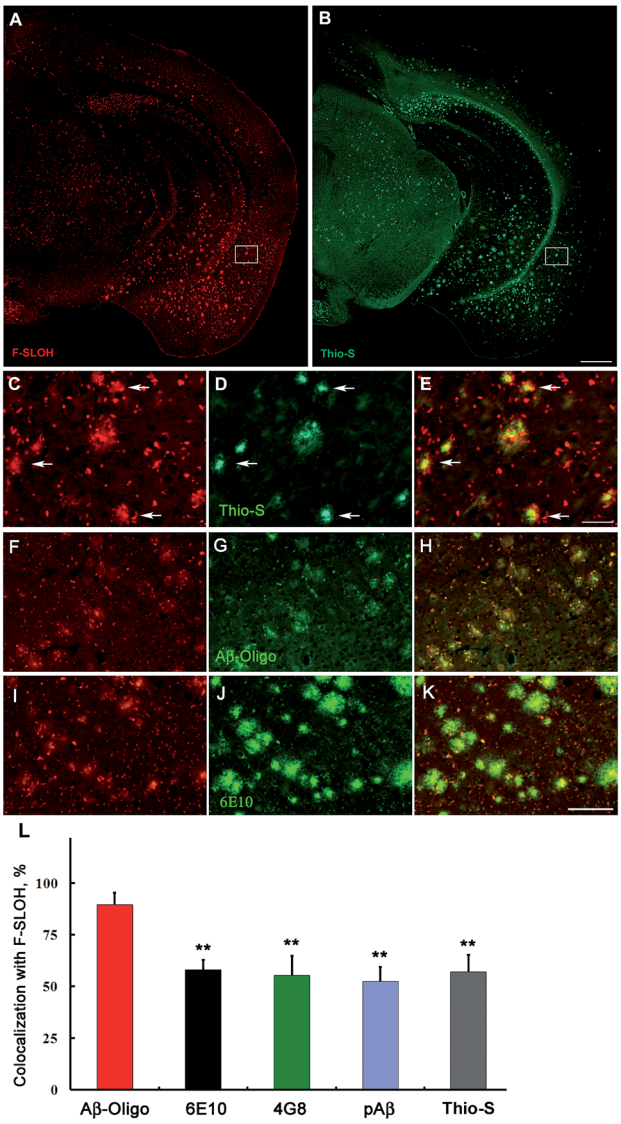

Fig. 4 Representative *in vivo* labelling of F-SLOH in AD Tg mouse models. F-SLOH was systemically administered in APP/PS1 double Tg or APP/PS1/Tau triple Tg mice. (A and B) F-SLOH *in vivo* labelling was examined by *ex vivo* imaging and co-staining with thioflavin-S (Thio-S). (C and D) Enlarged images of box frames in (A and B) respectively. (E) Merged images of (C and D). (F–K) *In vivo* F-SLOH labelled brain sections (F and I) were incubated with Aβ-Oligo or the 6E10 primary antibody followed by a secondary antibody conjugated with Alexa 488 (G and J). (H and K) Merged images of (F and G) and (I and J), respectively. Scale bar: 500 μm in (A and B), 200 μm in (C–K). (L) Quantitative analysis of co-localization between F-SLOH labelling *in vivo* and Aβ immunofluorescence or Thio-S staining *in vitro*. A percentage of the overlapping region to the total staining was adopted as an indicator for the extent of co-localization in each group. The area of the signals (% of the whole image) was quantified with ImageJ software on the images from the cortical region. Data are presented as the mean ± SD ($n = 4$); $^{**}P < 0.01$, *vs.* Aβ-Oligo group. The higher colocalization between F-SLOH labelling and Aβ-Oligo specific immunoreactivity *vs.* other antibodies or Thio-S staining suggests that F-SLOH targets the Aβ oligomers in the AD mouse brain *in vivo*.

higher fluorescence signals were consistently displayed in the Tg mouse compared to that of the WT mouse ($P < 0.05$) (Fig. S19B†). The longer retention of F-SLOH in the Tg mice further supported its strong interactions with Aβ species. Then, the brain slices of the F-SLOH-treated mice were harvested and imaged to further verify the brain penetration of F-SLOH. As shown in Fig. S20,† the plaque-enhanced F-SLOH fluorescence was clearly seen in the brain sections of the Tg mouse after 2 h of injection with a decreased intensity after 4 h of injection, whereas nearly no fluorescence signal was seen in the WT mouse after 2 h of injection. As compared with the reported oligomer probes, BD-Oligo and AN-SP, F-SLOH appears to have a much superior BBB penetrability.[22,23] To further investigate the targeting specificity of F-SLOH towards Aβ oligomers *in vivo*, the brain sections of the Tg mice were incubated with Thio-S and various antibodies. Consistently, Fig. 4 and Fig. S21† showed that *in vivo* labelling of F-SLOH displayed a highly similar pattern/result to that obtained from *in vitro* studies, and further quantitative analysis, shown in Fig. 4L, demonstrated that the extent of colocalization between F-SLOH and Aβ-Oligo reached approximately 90%, which is much higher than that of 6E10, 4G8, pAβ, or Thio-S (around 50–65%), affirming the specificity of F-SLOH to Aβ oligomers *in vivo*. Unlike other reported NIR imaging agents, F-SLOH was successfully applied to the *in vivo* detection of Aβ oligomers in the Tg mice at the young age of 7 months, at which age AD-like pathology is just forming at a relatively early stage in this model, highlighting its tremendous potential applications in the early diagnosis of AD.

Conclusions

In summary, we have developed a novel fluoro-substituted carbazole-based cyanine, namely F-SLOH, which exhibits a high binding affinity and selective recognition for Aβ oligomers over monomers and fibrils. The strong binding selectivity, as revealed by molecular docking simulation calculations, resulted from the synergistic effect of strong π–π stacking and intermolecular CH···O and CH···F bonding interactions between F-SLOH and the Aβ oligomer. These results highlight that the subtle structure modification (*i.e.* replacing H with an F atom) could cause dramatic changes in the functional and physical properties of a molecule. Importantly, F-SLOH also exhibited diverse desirable multifunctional properties for practical applications including excellent BBB penetrability, low bio-toxicity and strong fluorescence enhancement upon binding with Aβ oligomers. Remarkably, in addition to the good inhibitory effect on Aβ aggregation/fibrillogenesis, F-SLOH can protect Aβ-induced neuronal toxicity by means of inhibiting $[Ca^{2+}]$ elevation and ROS generation. Furthermore, *in vivo* imaging of 7 month-old AD mice models further confirmed that the probe could target Aβ oligomers and be washed out effectively from the brain. To the best of our knowledge, this is the first report on a theranostic probe that shows specific and effective *in vivo* labelling of Aβ oligomers and potent neuroprotective effects against Aβ-induced toxicities. This probe offers promising potential as a useful theranostic agent in early-stage diagnostics and therapeutics of AD.

Conflicts of interest

There are no conflicts to declare.

Acknowledgements

The authors acknowledge the financial support through the Cooperative Research Fund of Hong Kong Research Grant Council (C2012-15G), the Faculty Research Grant of Hong Kong Baptist University (FRG2/15-16/054), the General Research Fund (12301317), the 2014 Hong Kong Scholars Program, the China Postdoctoral Science Foundation funded project (2015M580685), the National Natural Science Foundation of China (21305036, 21675135, 30470594 and 30772282) and the Hunan Provincial Natural Science Foundation of China (2015JJ3035).

Notes and references

1 K. S. Kosik, *Science*, 1992, **256**, 780–783.
2 Y. Huang and L. Mucke, *Cell*, 2012, **148**, 1204–1222.
3 D. J. Selkoe, *Nat. Med.*, 2011, **17**, 1060–1065.
4 A. Abbott, *Nature*, 2008, **456**, 161–164.
5 J. A. Hardy and G. A. Higgins, *Science*, 1992, **256**, 184–185.
6 D. J. Selkoe, *Physiol. Rev.*, 2001, **81**, 741–766.
7 S. M. Ametamey, M. Honer and P. A. Schubiger, *Chem. Rev.*, 2008, **108**, 1501–1516.
8 M. M. Svedberg, O. Rahman and H. Hall, *Nucl. Med. Biol.*, 2012, **39**, 484–501.
9 S. Li, H. He, W. Cui, B. Gu, J. Li, Z. Qi, G. Zhou, C. M. Liang and X. Y. Feng, *Anat. Rec.*, 2010, **293**, 2136–2143.
10 M. Cui, M. Ono, H. Watanabe, H. Kimura, B. Liu and H. Saji, *J. Am. Chem. Soc.*, 2014, **136**, 3388–3394.
11 C. H. Heo, A. R. Sarkar, S. H. Baik, T. S. Jung, J. J. Kim, H. Kang, I. Mook-Jung and H. M. Kim, *Chem. Sci.*, 2016, **7**, 4600–4606.
12 J. Hardy and D. J. Selkoe, *Science*, 2002, **297**, 353–356.
13 M. Goedert and M. G. Spillantini, *Science*, 2006, **314**, 777–781.
14 B. Caughey and P. T. Lansbury, *Annu. Rev. Neurosci.*, 2003, **26**, 267–298.
15 C. Haass and D. J. Selkoe, *Nat. Rev. Mol. Cell Biol.*, 2007, **8**, 101–112.
16 K. L. Viola and W. L. Klein, *Acta Neuropathol.*, 2015, **129**, 183–206.
17 P. N. Lacor, M. C. Buniel, L. Chang, S. J. Fernandez, Y. Gong, K. L. Viola, M. P. Lambert, P. T. Velasco, E. H. Bigio, C. E. Finch, G. A. Krafft and W. L. Klein, *J. Neurosci.*, 2004, **24**, 10191–10200.
18 M. Cui, *Curr. Med. Chem.*, 2014, **21**, 82–112.
19 I. W. Hamley, *Chem. Rev.*, 2012, **112**, 5147–5192.
20 K. L. Viola, J. Sbarboro, R. Sureka, M. De, M. A. Bicca, J. Wang, S. Vasavada, S. Satpathy, S. Wu, H. Joshi, P. T. Velasco, K. MacRenaris, E. A. Waters, C. Lu, J. Phan, P. Lacor, P. Prasad, V. P. Dravid and W. L. Klein, *Nat. Nanotechnol.*, 2015, **10**, 91–98.
21 V. Ntziachristos, *Annu. Rev. Biomed. Eng.*, 2006, **8**, 1–33.
22 C. L. Teoh, D. Su, S. Sahu, S. W. Yun, E. Drummond, F. Prelli, S. Lim, S. Cho, S. Ham, T. Wisniewski and Y. T. Chang, *J. Am. Chem. Soc.*, 2015, **137**, 13503–13509.
23 G. Lv, A. Sun, P. Wei, N. Zhang, H. Lan and T. Yi, *Chem. Commun.*, 2016, **52**, 8865–8868.
24 W. Yang, Y. Wong, O. T. W. Ng, L. P. Bai, D. W. J. Kwong, Y. Ke, Z. H. Jiang, H. W. Li, K. K. L. Yung and M. S. Wong, *Angew. Chem., Int. Ed.*, 2012, **51**, 1804–1810.
25 Y. Li, D. Xu, S. L. Ho, H. W. Li, R. Yang and M. S. Wong, *Biomaterials*, 2016, **94**, 84–92.
26 L. Zhu, Y. Song, P.-N. Cheng and J. S. Moore, *J. Am. Chem. Soc.*, 2015, **137**, 8062–8068.
27 K. N. Dahlgren, A. M. Manelli, W. B. Stine, L. K. Baker, G. A. Krafft and M. J. LaDu, *J. Biol. Chem.*, 2002, **277**, 32046–32053.
28 L. Zhu, Y. Song, P.-N. Cheng and J. S. Moore, *J. Am. Chem. Soc.*, 2015, **137**, 8062–8068.

